Supporting Information

Reconfigurable band alignment of SeWS/h-BP van der Waals heterostructures for photoelectric applications

Dong Wei[1], Yi Li[2], Gaofu Guo[1], Heng Yu[1], Yaqiang Ma[1], Yanan Tang[2], and Xianqi Dai[1,*]

[1] School of Physics, Henan Normal University, Xinxiang, Henan 453007, China.

[2] School of Physics and Electronic Engineering, Zhengzhou Normal University, Zhengzhou, Henan 450044, China.

With various stacking orders, the SeWS and h-BP single layer can form different heterobilayer structures, which are labeled by A, B, C, D, E, and F. The D, E and F configurations are obtained by rotating h-BP layer 180◦ around the vertical axis of the A, B and C type structures, respectively. The a-f configuration is similar to the A-F configuration, the only difference is the contact surface between the SWSe layer and the h-BP layer.

* Address correspondence to E-mail: xqdai@htu.cn (Xianqi Dai).

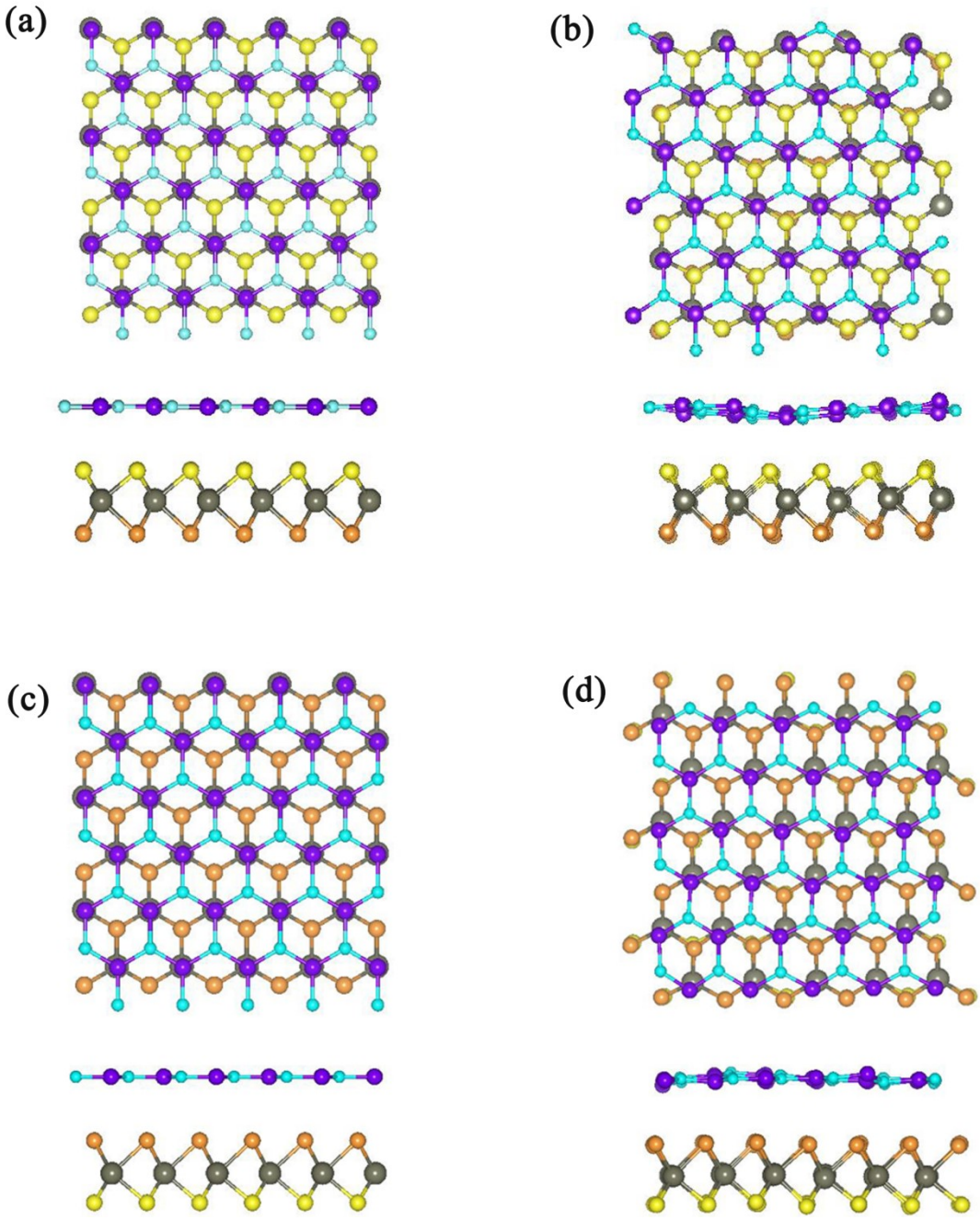

Fig. S1. The (a), (b), (c) and (d) are schematic diagrams of the structures of SeWS/h-BP and SWSe/h-BP vdWHs before and after the AIMD simulation, respectively.

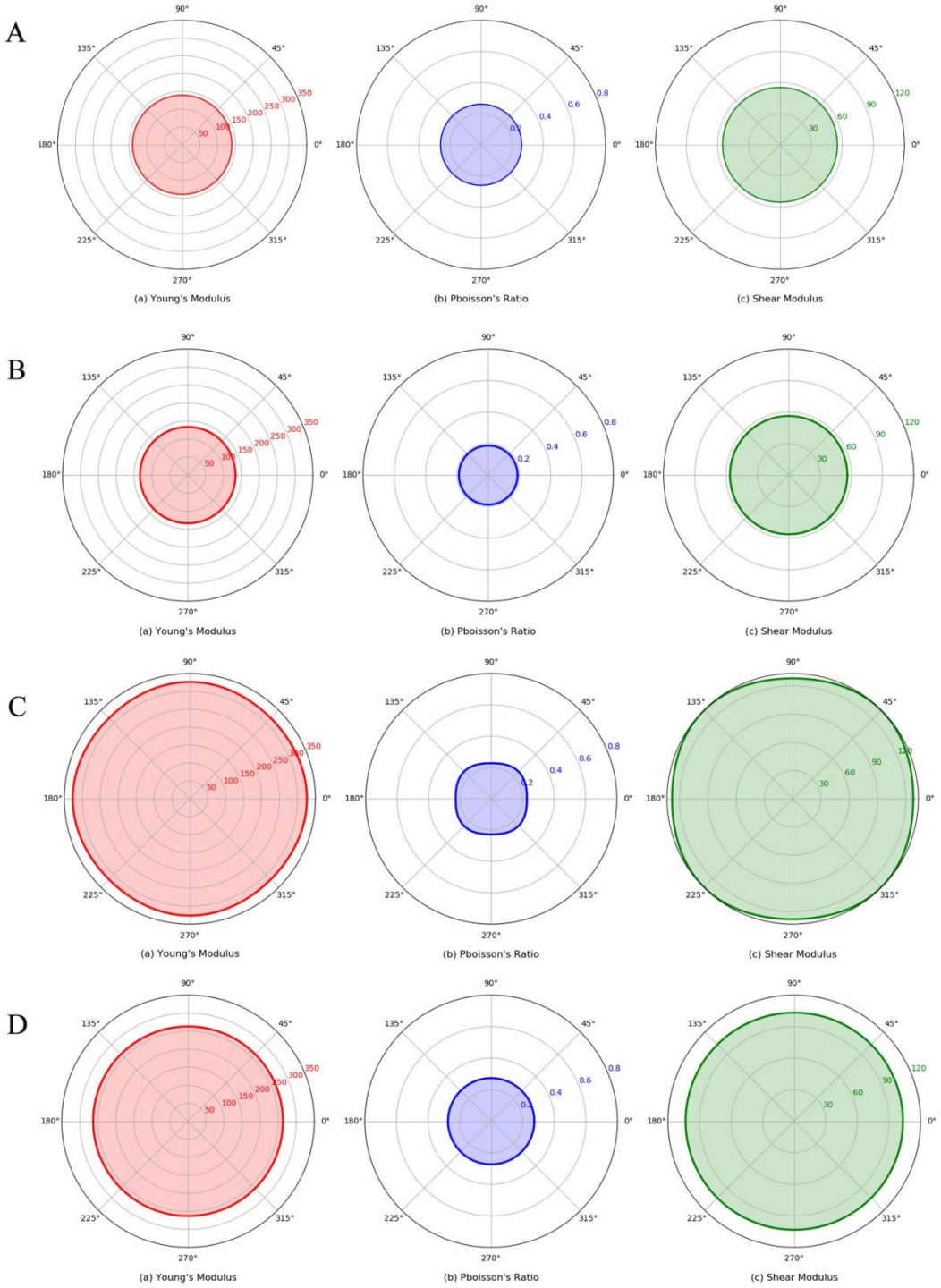

Fig. S2. The A, B, C and D are the h-BP, SeWS monolayers, SeWS/h-BP and SWSe/h-BP vdWHs, respectively. The perfect circlarity means the vdWHs have perfectly isotropic elastic properties.

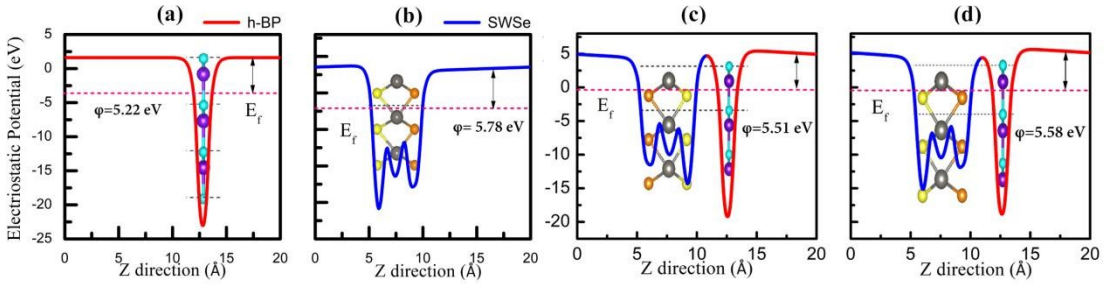

Fig. S3. The average electrostatic potential for the (a) h-BP and (b) SWSe monolayer, (c) SeWS/h-BP and (d) SWSe/h-BP vdWHs, respectively.

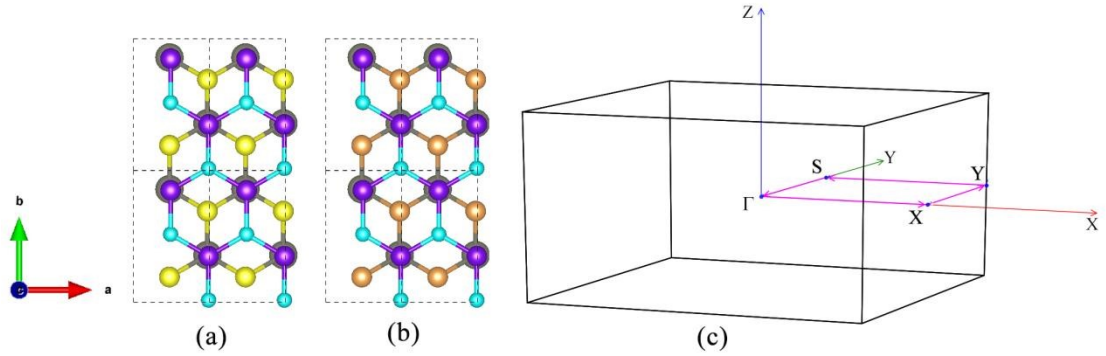

Fig. S4. The (a) and (b) are the orthogonal lattice of SeWS/h-BP and SWSe/h-BP vdWHs, respectively. (c) In the first Brillouin zone, the orthogonal supercell has been presented by the pink line with points Γ, X, Y, and S.

To study the mobility properties of electrons and holes, the carrier mobility μ_{2D} of the 2D semiconducto can be obtained as follows:

$$\mu_{2D} = \frac{e\hbar^3 C_{2D}}{K_B T m^* m_d E_1^2}$$

(2)

where e is the electron charge, $\hbar$ is the reduced Planck constant, K_B is the Boltzmann constant and T is the temperature(300 K in our calculations). The m^* and $m_d = \sqrt{m_x^* m_y^*}$ are the effective mass and average effective mass of carriers along the transport direction, respectively. The in-plane stiffness $C_{2D} = 2[\partial^2 E/\partial(\Delta l/l_0)^2]/S_0$, where the E is total energy and S_0 is the area of the vdWHs. The $E_1 = \Delta V/(\Delta l/l_0)$ is the deformation potential constant, the $\Delta V = \Delta E_{VBM}$ or ΔE_{CBM} (strain range from -2% to 2%, calculated using 0.5% steps), Δl and l_0 are the deformation of the lattice constants

along the transport direction and the intrinsic lattice constants, correspondingly.

Here, the effective masses and mobilities of carriers along the *x* and *y* directions were calculated, in which the orthorhombic lattices were used instead of the hexagonal cells for intrinsic h-BP, SeWS layers and SeWS/h-BP (SWSe/h-BP) vdWHs.

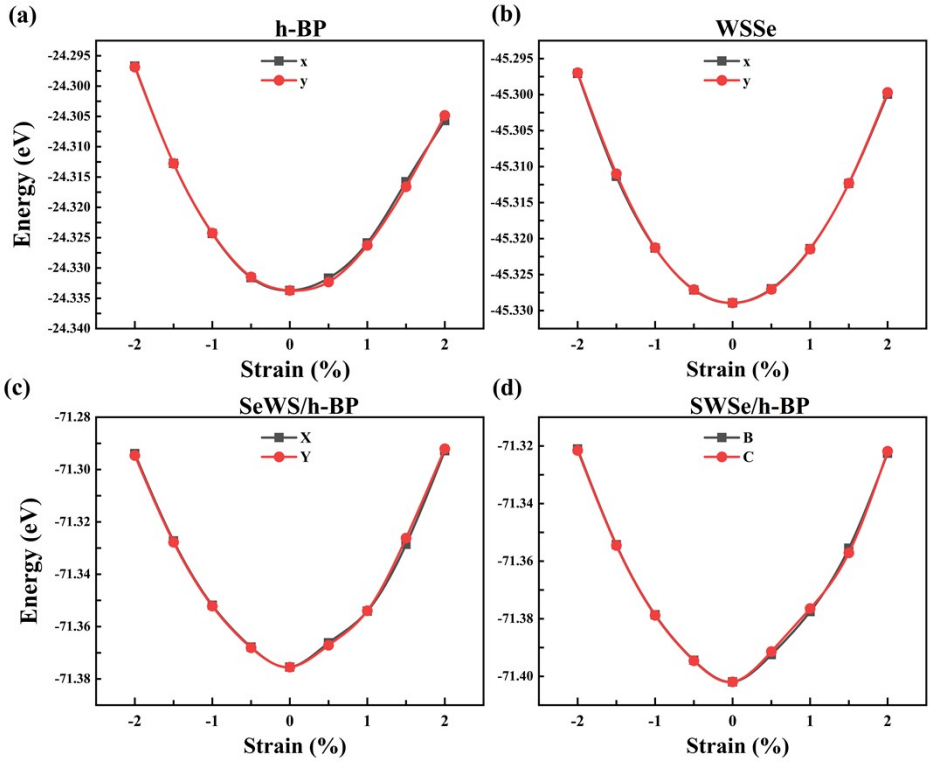

Fig. S5. The (a), (b), (c) and (d) are the change of total energy for h-BP, WSSe, SeWS/h-BP vdWHs and SWSe/h-BP vdWHs at -2%-2% uniaxial strain, respectively.

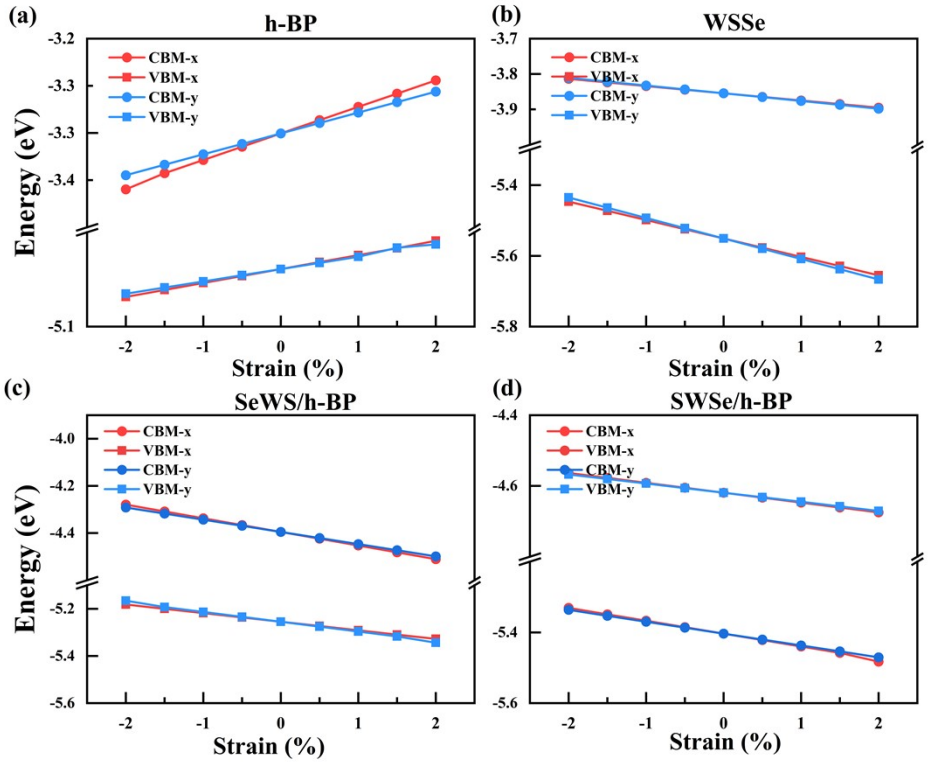

Fig. S6. The (a), (b), (c) and (d) are the variation of VBM and CBM energy positions at -2%-2% uniaxial strain for h-BP, WSSe, SeWS/h-BP vdWHs and SWSe/h-BP vdWHs , respectively.

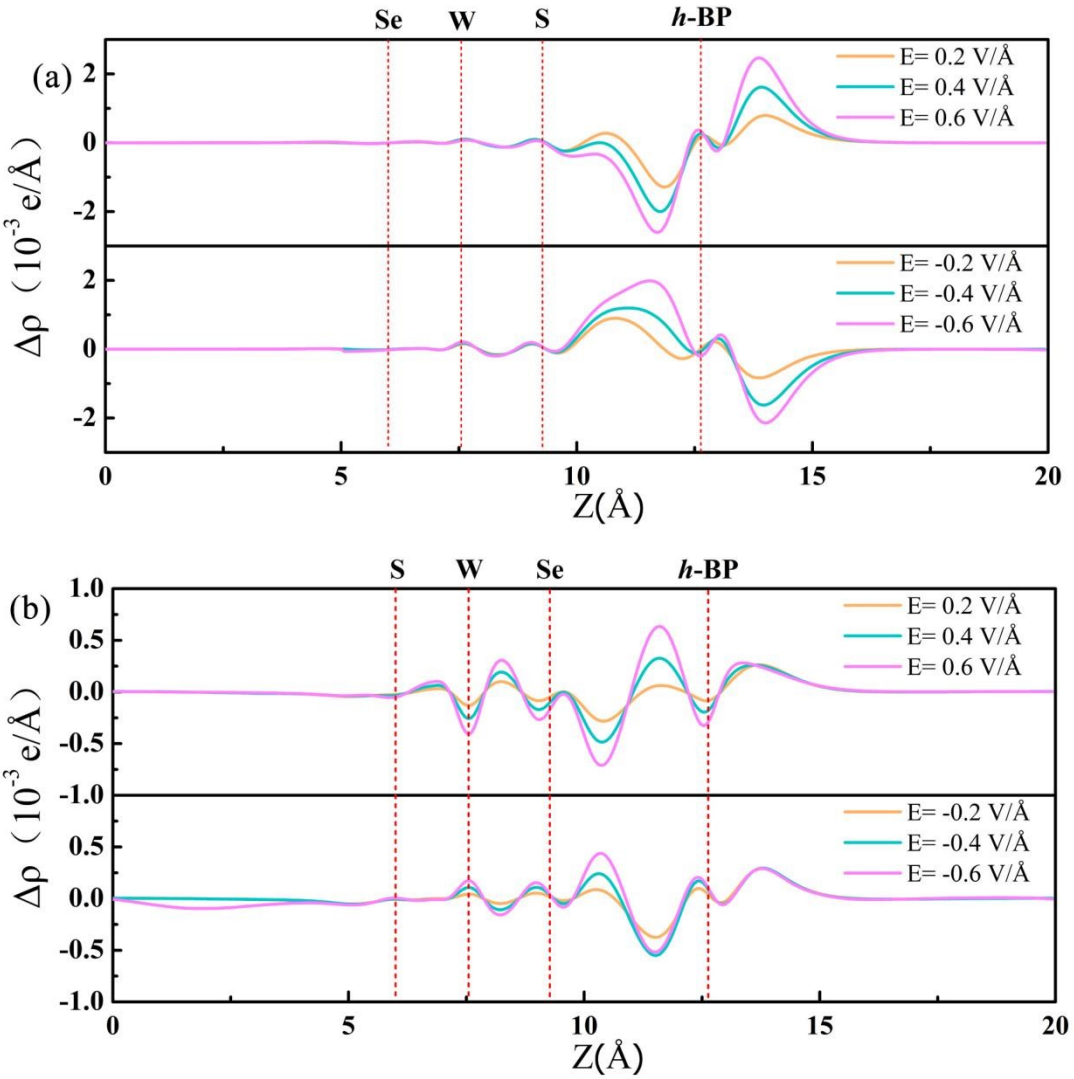

Fig. S7. The integrated charge density difference in (a) S and Se vdWHs with various E_{field} along *z* direction.

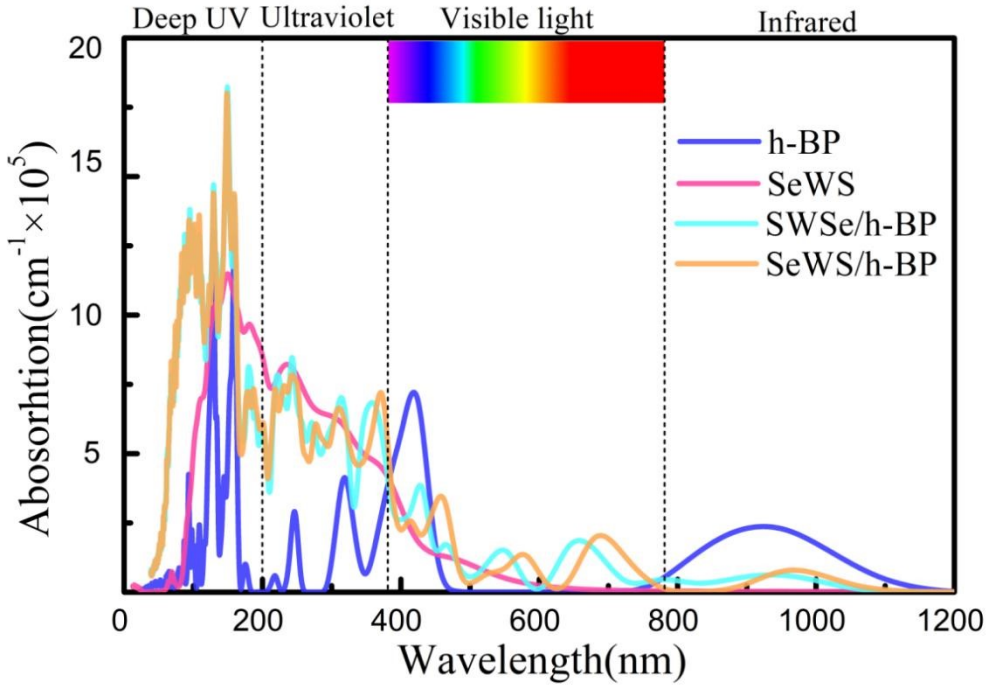

Fig. S8. The optical absorption coefficient of the h-BP layer, SeWS layer, SWSe/h-BP and SeWS/h-BP vdWHs.

To explore the optical properties, the frequency-dependent dielectric function [ε(ω)] was calculated and obtained the optical absorption coefficient α(ω) according to the following equation:

$$\alpha = \sqrt{2}\omega\sqrt{\left(\sqrt{\varepsilon_1^2(\omega) + \varepsilon_2^2(\omega)} - \varepsilon_1(\omega)\right)} \quad (1)$$

where $\varepsilon_1(\omega)$ and $\varepsilon_2(\omega)$ are the real and imaginary parts of the complex dielectric function, respectively.

Table S1. The elastic constants of C_{11},C_{12} and C_{66} (N m^{-1}), the Young's modulus Y (N m^{-1}) and Poisson ratio v.

	C_{11}	C_{12}	C_{66}	Y	v
h-BP	149.564	38.999	55.283	139.395	0.26
SeWS	138.511	25.980	56.265	133.683	0.19
SeWS/h-BP	334.023	78.118	127.952	315.753	0.23
SWSe/h-BP	284.206	77.725	103.24	262.950	0.27

The power conversion efficiency equation:

$$\eta = \frac{J_{SC} V_{OC} \beta_{FF}}{P_{solar}} = \frac{0.65(E_g - \Delta E_c - 0.3) \int_{E_g}^{\infty} P(\hbar\omega) EQE(\hbar\omega)}{\int_{0}^{\infty} P(\hbar\omega) d(\hbar\omega)} \quad (2)$$

where 0.65 is the band-fill factor (β_{FF}), E_g is the bandgap of the donor, ΔE_c is the conduction band offset (CBO) at the Anderson Limit. The term ($E_g - \Delta E_c - 0.3$) evaluates the maximum open circuit voltage V_{oc}, where 0.3 eV is an empirical factor that has been discussed. The $P(\hbar\omega)$ denotes the AM 1.5 solar energy flux (W m^{-2} eV^{-1}) with $\hbar\omega$ of phono energy. The integral in the numerator represents the short-circuit current *Jsc*, assuming 100% external quantum efficiency (EQE), the P_{solar} is the total incident solar power per area at AM 1.5. The E_g is regarded as the lower limit of integration of the term $\int_{E_g}^{\infty} P(\hbar\omega) EQE(\hbar\omega)$, where the electrons can be excited into a higher level after absorbing photon energy over E_g.